AIMS Mathematics, 10(8): 17954–17981.
DOI:10.3934/math.2025800
Received: 21 April 2025
Revised: 21 July 2025
Accepted: 30 July 2025
Published: 07 August 2025

https://www.aimspress.com/journal/Math

Research article

Theoretical study of interval-valued fuzzy cognitive maps: inference mechanisms, convergence, and centrality measures

Jindong Feng[1,2] **and Zengtai Gong**[1,*]

[1] College of Mathematics and Statistics, Northwest Normal University, Lanzhou 730070, China

[2] College of Mathematics and Computer Science, Northwest Minzu University, Lanzhou 730030, China

* **Correspondence:** Email: zt-gong@163.com.

Abstract: Fuzzy cognitive maps (FCMs) have garnered significant attention for modeling and analyzing complex systems, owing to their ability to effectively handle uncertainty and nonlinear relationships. Interval-valued fuzzy cognitive maps (IVFCMs), as an extension of FCMs, further enhance this capability by incorporating interval-valued fuzzy numbers to better represent system uncertainty and complexity. Despite their potential, most existing research on IVFCMs has focused on applications, with limited advancement in their theoretical foundations. This study established a comprehensive theoretical framework for IVFCMs, addressing critical gaps in their mathematical basis and dynamic behavior. The key contributions are as follows: (1) Formalization of the inference mechanism, including a rigorous definition of state updates using interval-valued fuzzy operations, and a proof that IVFCMs reduce to conventional FCMs as interval widths approach zero; (2) establishment of convergence guarantees by deriving sufficient stability conditions through spectral radius analysis and the Banach fixed-point theorem for sigmoid activation functions; (3) the proposal of novel centrality measures, introducing interval-valued degree and closeness centrality, supported by an optimized Dijkstra algorithm for efficient identification of key nodes; and (4) empirical validation through a time series prediction case study, demonstrating the model's superior performance in managing uncertainty and noise across different datasets. Overall, this work addressed fundamental theoretical challenges related to inference, convergence, and structural analysis in IVFCMs, while also demonstrating their practical utility in complex system modeling.

Keywords: interval operation; interval-valued fuzzy cognitive maps; complex systems modeling; inference mechanisms; convergence; centrality measurement
Mathematics Subject Classification: 03B52, 05C72

1. Introduction

Fuzzy cognitive maps (FCMs), first introduced by Kosko in 1986 [1], serve as a powerful tool for knowledge representation and inference. By integrating fuzzy logic, graph theory, and cognitive science, FCMs provide a robust framework for addressing knowledge processing challenges in complex systems. They represent knowledge in an intuitive graphical format, facilitating both its storage and retrieval. In this framework, nodes represent specific concepts—for example, species population and environmental temperature in ecological studies, or inflation and unemployment rates in economic systems. Directed edges between nodes capture causal relationships, with associated weights indicating the strength and direction of these influences. This structure enables the modeling of intricate interdependencies within complex domains [2]. For inference, FCMs utilize iterative computations to simulate state transitions over time or under changing conditions, based on the fuzzy causal relationships among nodes. This mechanism allows FCMs to manage uncertainty effectively, thereby improving the accuracy and robustness of the inference process.

Due to their strong modeling capabilities, interpretability, and flexibility, FCMs have been widely applied in various domains, including environmental science [3], medical assistive systems [4], financial decision-making [5], crisis management [6, 7], and time series analysis [8]. However, most existing studies have primarily focused on the practical applications of FCMs, while theoretical investigations remain relatively limited. For instance, Choukolaei et al. [6] proposed a hybrid framework integrating FCMs and the PROMETHEE method to enhance relief center selection by modeling criterion interdependencies and spatial constraints, thereby supporting earthquake-resilient urban planning. The literature [7] employed FCMs to evaluate the weight and impact of individual risks, utilizing expert input to define causal relationships and calculate centrality indices. Their approach addressed critical gaps in dynamic risk assessment and relief demand estimation, offering valuable insights for crisis management. Departing from research that applies fuzzy cognitive mapping to practical problems, this study develops extensions to FCMs' mathematical foundations for enhanced uncertainty modeling. Current theoretical research on FCMs mainly addresses three core areas: (1) the convergence and stability of FCM models, (2) the centrality measures of FCMs, and (3) the development of extended FCM frameworks.

Studies on convergence and stability typically examine FCMs equipped with continuous, non-decreasing, and nonlinear activation functions—most commonly, the sigmoid function. This line of research investigates the dynamic behavior of FCM systems and establishes sufficient conditions for the existence and uniqueness of fixed points. Boutalis et al. [9] employed the contraction mapping theorem and the non-expansive mapping theorem to analyze the concept value equations of FCMs and derived conditions ensuring a unique solution. They further demonstrated the stability of the adaptive weight estimation algorithm and the convergence of parameters by constructing a Lyapunov function. Building on this work, Kottas et al. [10] extended the conditions for the existence and uniqueness of equilibrium points by jointly considering the weights and the slope parameters of the sigmoid function. They proposed a bilinear adaptive estimation algorithm to enhance the structural flexibility and adaptability of FCMs. Knight et al. [11] utilized the Taylor expansion, the implicit function theorem, and the Jacobian matrix to analyze the properties of fixed points in sigmoid-based FCMs. Nápoles et al. [12] introduced a heuristic algorithm aimed at improving convergence in pattern classification tasks, which was further optimized and validated through simulations using the

particle swarm optimization algorithm. Luo et al. [13] applied the semi-tensor product technique to transform K-valued FCMs into an algebraic representation, providing a general formula for computing the number of fixed points and limit cycles. Harmati et al. [14] established conditions for the global stability of FCMs through theoretical derivations based on the induced matrix norm and spectral radius.

Centrality measures, a fundamental analytical tool in graph theory, quantify the relative importance of nodes within a network's structure. By systematically identifying influential nodes, these measures provide insights into critical aspects such as information dissemination, resource allocation, and network stability. Foundational indices like degree centrality and closeness centrality, introduced in Freeman's seminal work [15], have laid the groundwork for the analysis of complex networks. As centrality theory has evolved through interdisciplinary integration, a variety of computational methods have emerged, enabling applications across diverse domains—including social network analysis [16], biological network modeling [17], and communication network optimization [18]. In the context of fuzzy complex networks, Hu et al. [19] evaluated multiple centrality measures in directed fuzzy social networks, analyzing their means and variances. Lu et al. [20] developed a centrality analysis model for fuzzy social networks to uncover the characteristics of interpersonal nodes and their interrelationships in online platforms. Obiedat et al. [21] employed a 2-tuple fuzzy linguistic representation to handle imprecise linguistic and numerical data, proposing a consensus-based centrality measure for assessing node importance in FCMs. Wang et al. [22] constructed a fuzzy social network model grounded in fuzzy hypergraph theory and introduced corresponding structural centrality measures to more accurately identify key members within the network.

In parallel, several extended FCM models have been proposed to more effectively address uncertainty, multi-scale complexity, and nonlinear system behavior. For example, high-order fuzzy cognitive maps (HFCMs) [23–25] enable multiple nodes to jointly influence a target node through combinational mechanisms, thereby capturing higher-order relationships and complex causal chains. Intuitionistic fuzzy cognitive maps (IFCMs) [26] incorporate intuitionistic fuzzy sets—characterized by degrees of membership, non-membership, and hesitation—to enhance the representation of uncertainty in both concept states and causal links. Fermatean fuzzy cognitive maps (FFCMs) [27] incorporate Fermatean fuzzy numbers to represent the causal weights (edges) and the activation levels of concepts (nodes).

Interval-valued fuzzy cognitive maps (IVFCMs) [28] utilize interval-valued fuzzy numbers to represent node states and edge weights, providing improved handling of imprecise information. Meanwhile, dynamic fuzzy cognitive maps (DFCMs) [29] integrate temporal variables, allowing concept states to evolve over time and more accurately capture the dynamic behavior of complex systems.

Among the various extensions of FCMs, IVFCMs significantly enhance the ability to model complex systems. First, IVFCMs improve the quantification of uncertainty. By replacing single-valued weights with interval values, they incorporate diverse expert opinions, reduce noise interference, and more effectively capture the fuzzy nature and inherent uncertainty of causal relationships. Second, IVFCMs increase the flexibility and dynamic adaptability of knowledge representation. The interval-based multi-granularity framework enables IVFCMs to simultaneously express both "conservative" and "aggressive" estimates within a single model. For example, in medical diagnosis, the causal relationship between a symptom and a disease may vary due to individual differences; interval values offer a flexible means to accommodate such variability. This interval evolution mechanism

also facilitates parameter adjustment during dynamic transitions, allowing for a more accurate representation of system progression from transient to steady states.

When intervals are introduced to handle uncertainty in IVFCMs, the selection of an appropriate interval arithmetic method becomes crucial. Interval arithmetic is a mathematical framework that operates on intervals—defined as pairs of numbers representing lower and upper bounds—rather than on precise values. This method ensures rigorous tracking of uncertainty and rounding errors throughout computations. Hickey et al. [30] established a rigorous mathematical foundation for interval arithmetic, starting from the definition of real intervals as closed, connected sets of reals. Deschrijver [31] introduced novel arithmetic operators (addition, subtraction, multiplication, division) for the lattice $\mathcal{L}^I$ (the underlying structure of interval-valued fuzzy sets and intuitionistic fuzzy sets). These operators extend classical fuzzy arithmetic to handle intervals while preserving key algebraic properties. Piegat et al. [32] proposed a decomposition approach that splits type-2 intervals into inner (high-credibility) and outer (global) type-1 intervals. Arithmetic operations (e.g., addition) of this approach yield multidimensional solution sets (not single intervals), enabling higher accuracy. Breiding et al. [33] used interval arithmetic and Krawczyk's method to certify isolated nonsingular zeros of polynomial systems.

Despite its numerous advantages, current research on IVFCMs still encounters three fundamental theoretical challenges that hinder its effective implementation:

1) Inference mechanism gaps: The mathematical foundations of interval-valued operations in state transitions lack formal analysis, particularly regarding the preservation of interval properties during iterative updates.

2) Convergence uncertainties: Stability conditions for IVFCMs remain unexplored, with no established theoretical guarantees that interval-valued systems will converge to equilibrium states.

3) Centrality measurement limitations: Existing graph centrality metrics cannot directly handle interval-valued weights, creating challenges for identifying influential nodes in IVFCM networks.

This study systematically addresses these gaps by establishing a comprehensive theoretical framework for IVFCMs. First, we formalize the inference mechanism through interval arithmetic operations and demonstrate how IVFCMs reduce to conventional FCMs when interval widths approach zero (Theorem 3). Second, we derive sufficient convergence conditions using the Banach fixed-point theorem and spectral radius analysis (Theorem 5), providing practical design constraints for stable systems. Finally, we develop novel interval-valued centrality measures (Definitions 6–8) with optimized path-search algorithms for efficient computation. By resolving these theoretical challenges, our work enables more reliable deployment of IVFCMs in complex real-world applications where uncertainty quantification is critical.

The remainder of this paper is organized as follows: Section 2 reviews the preliminary concepts related to IVFCMs. Section 3 examines the inference mechanism of IVFCMs. Section 4 investigates their convergence properties and proposes a sufficient condition for convergence. Section 5 introduces two centrality measures designed for IVFCMs. Section 6 presents a case study on time series prediction. Finally, Section 7 offers concluding remarks and outlines directions for future research.

2. Preliminaries

An interval number is typically expressed as $[a, b]$, where a and b are real numbers satisfying $a \leq b$. It represents a numerical range encompassing all values between a and b. As a fundamental mathematical tool, an interval number provides an intuitive approach to representing uncertainty by defining a range of possible values rather than a single fixed value. This concept is widely applied in interval-valued fuzzy sets and IVFCMs, enabling more effective modeling of uncertainty and complexity in real-world problems. The following section introduces key definitions and fundamental concepts relevant to this research.

Definition 1. *[34] Let X be the universe of discourse. An interval-valued fuzzy set $\tilde{A}$ on X is defined as: $\tilde{A} = \left\{\left(x, \left[\mu^-_{\tilde{A}}(x), \mu^+_{\tilde{A}}(x)\right]\right) \mid x \in X\right\}$, where $\mu^-_{\tilde{A}}(x)$ and $\mu^+_{\tilde{A}}(x)$ represent the lower membership function and the upper membership function of the element x in the interval-valued fuzzy set $\tilde{A}$, respectively, and satisfy $0 \leqslant \mu^-_{\tilde{A}}(x) \leqslant \mu^+_{\tilde{A}}(x) \leqslant 1$.*

Definition 2. *[34] Let $\tilde{A}$ and $\tilde{B}$ be two interval-valued fuzzy sets on the universe of discourse X. Then $\tilde{A} \subseteq \tilde{B}$ if and only if for any $x \in X$, $\mu^-_{\tilde{A}}(x) \leqslant \mu^-_{\tilde{B}}(x)$ and $\mu^+_{\tilde{A}}(x) \leqslant \mu^+_{\tilde{B}}(x)$.*

Definition 3. *[31] For two interval-valued fuzzy sets $\tilde{A}$ and $\tilde{B}$ on the universe of discourse X, their addition and multiplication operations are defined as follows:*

$$\tilde{A} \oplus \tilde{B} = \left[\min\left(\mu^-_{\tilde{A}}(x) + \mu^+_{\tilde{B}}(x), \mu^+_{\tilde{A}}(x) + \mu^-_{\tilde{B}}(x)\right), \mu^+_{\tilde{A}}(x) + \mu^+_{\tilde{B}}(x)\right], \tag{2.1}$$

$$\tilde{A} \otimes \tilde{B} = \left[\mu^-_{\tilde{A}}(x)\mu^-_{\tilde{B}}(x), \max\left(\mu^-_{\tilde{A}}(x)\mu^+_{\tilde{B}}(x), \mu^+_{\tilde{A}}(x)\mu^-_{\tilde{B}}(x)\right)\right]. \tag{2.2}$$

Interval-valued fuzzy sets generalize traditional fuzzy sets by representing membership degrees as intervals rather than single values. This extension captures epistemic uncertainty—situations where experts specify ranges (e.g., "this symptom indicates Disease A with 60–70% confidence") due to incomplete knowledge or conflicting evidence. The selection of specific interval operations ($\oplus$ and $\otimes$) is guided by three requirements for uncertainty propagation: Completeness: results must encompass all possible values arising from input combinations. Conservatism: bounds should reflect worst-case and best-case scenarios. Interpretability: outputs must align with real-world decision-making contexts.

For the $\oplus$ (addition) operation, which models aggregated influences (e.g., combining risk factors), the lower bound represents pessimistic combinations (the minimum of all possible pairwise sums), while the upper bound represents optimistic scenarios (the sum of the individual maxima). For the $\otimes$ (multiplication) operation, which models chained causalities (e.g., A causes B, which then affects C), the lower bound assumes minimal reinforcement (the minimum possible product of influences), while the upper bound considers maximal amplification (the maximum of all possible pairwise products).

Theorem 1. *Let $\tilde{A}$ and $\tilde{B}$ be two interval-valued fuzzy sets on the universe of discourse X. Then $\tilde{A} \otimes \tilde{B}$ is still an interval-valued fuzzy set on the universe of discourse X.*

Proof. According to Definitions 1 and 3, it is necessary to verify the following two points:

(1) The lower bound $\leq$ the upper bound:

Since $\mu^-_{\tilde{A}}(x) \leq \mu^+_{\tilde{A}}(x)$ and $\mu^-_{\tilde{B}}(x) \leq \mu^+_{\tilde{B}}(x)$, then:

$$\mu^-_{\tilde{A}}(x) \cdot \mu^-_{\tilde{B}}(x) \leq \mu^-_{\tilde{A}}(x) \cdot \mu^+_{\tilde{B}}(x) \quad \text{and} \quad \mu^-_{\tilde{A}}(x) \cdot \mu^-_{\tilde{B}}(x) \leq \mu^+_{\tilde{A}}(x) \cdot \mu^-_{\tilde{B}}(x).$$

Therefore, the lower bound ≤ the upper bound (because the upper bound is the larger one of the two values).

(2) The interval values are within [0, 1]:

All product terms are non-negative numbers (the membership degree ∈ [0, 1]), and:

$$\mu_{\tilde{A}}^{-}(x) \cdot \mu_{\tilde{B}}^{-}(x) \leq \max\left(\mu_{\tilde{A}}^{-}(x) \cdot \mu_{\tilde{B}}^{+}(x), \mu_{\tilde{A}}^{+}(x) \cdot \mu_{\tilde{B}}^{-}(x)\right) \leq 1.$$

□

Theorem 1 demonstrates that the multiplication of interval-valued fuzzy sets is a closed operation. However, it is evident that the addition of interval-valued fuzzy sets does not exhibit this property.

The construction of IVFCMs follows a similar process to that of traditional FCMs. The key distinction is that IVFCMs represent concept node values and edge weights using interval values rather than single fuzzy values. By adapting the iterative equation of traditional FCMs and incorporating the addition and multiplication operators for interval-valued fuzzy sets, as defined in Definition 3, the inference equation for IVFCMs is formulated as follows.

Definition 4. *[28] For any concept node A_j in an interval-valued fuzzy cognitive map (IVFCM), its state value at iteration $t+1$, denoted as $A_j(t+1)$, is updated using the following equation:*

$$\left\{\left[x^L, x^U\right]\right\}_j^{t+1} = f\left(\bigoplus_{\substack{i=1 \\ i\neq j}}^{N} \left\{\left[w^L, w^U\right]\right\}_{ij} \otimes \left\{\left[x^L, x^U\right]\right\}_i^t\right), \tag{2.3}$$

where N is the number of concepts, f is the activation function, $\left\{\left[x^L, x^U\right]\right\}_i^t$ represents the interval-valued fuzzy state of concept node A_i at time t with $0 \leq x^L \leq x^U \leq 1$, and $\{[w^L, w^U]\}_{ij}$ denotes the weight between concepts i and j with $-1 \leq w^L \leq w^U \leq 1$.

If the past activation value of a concept node is also considered in addition to the influence of other concepts, the state update equation is modified as follows:

$$\left\{\left[x^L, x^U\right]\right\}_j^{t+1} = f\left(\left(\bigoplus_{\substack{i=1 \\ i\neq j}}^{N} \left\{\left[w^L, w^U\right]\right\}_{ij} \otimes \left\{\left[x^L, x^U\right]\right\}_i^t\right) \oplus \left\{\left[x^L, x^U\right]\right\}_j^t\right). \tag{2.4}$$

In IVFCMs, edge weights describe the magnitude and direction of causal influence between concepts. If both w^L and w^U are positive, the influence is positive; if both are negative, the influence is negative. The addition ($\oplus$) and multiplication ($\otimes$) operators are defined in Definition 3. The activation function f is typically a monotonically non-decreasing nonlinear function, such as the sigmoid function commonly used in machine learning. Its primary role is to map the weighted summation results into a suitable range, ensuring the validity and interpretability of the concept values.

3. The inference mechanism of interval-valued fuzzy cognitive maps

Similar to conventional FCMs, the inference process of IVFCMs is carried out through iterative computation. A distinguishing feature of IVFCMs is that both the state values of concept nodes and the

edge weights representing causal relationships are expressed as interval numbers. The process begins with the initialization of all concept nodes and their corresponding state values, which represent the system's current status or the degree of activation for each concept. At the same time, the interval-valued edge weights—indicating the strength of causal influences—are determined either through expert judgment or data-driven optimization methods. Using the current node states and interval weights, an iterative algorithm updates the states of all nodes at each time step until the system reaches a stable state or satisfies predefined termination criteria. By observing the evolution of node states throughout the iterations, one can infer the underlying causal relationships and dynamic behavior of the system. To illustrate this inference process, a simple economic system example is presented in this subsection.

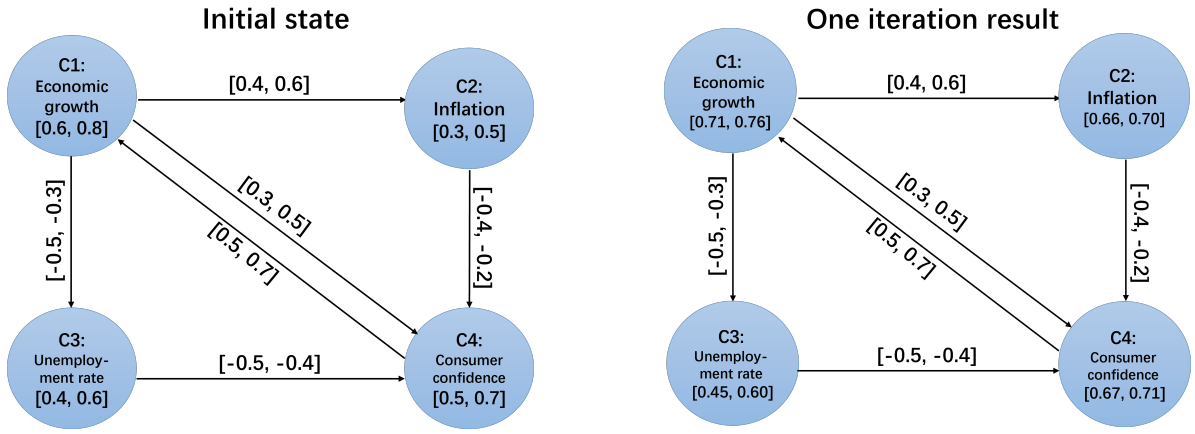

Figure 1. A simple example of an IVFCM about an economic system.

Example 1. *Figure 1 illustrates the first iteration of inference in an IVFCM applied to an economic system. As shown in the figure, the model consists of four concept nodes: economic growth (C_1), inflation (C_2), unemployment rate (C_3), and consumer confidence (C_4). The initial activation vector is given by:*

$$A^{(0)} = ([0.6, 0.8], [0.3, 0.5], [0.4, 0.6], [0.5, 0.7]).$$

The corresponding weight matrix for this IVFCM is defined as follows:

$$W = \begin{pmatrix} 0 & [0.4, 0.6] & [-0.5, -0.3] & [0.3, 0.5] \\ 0 & 0 & 0 & [-0.4, -0.2] \\ 0 & 0 & 0 & [-0.5, -0.4] \\ [0.5, 0.7] & 0 & 0 & 0 \end{pmatrix}.$$

Following Eq (2.4), the first iteration of inference in this IVFCM is carried out. The activation function f is the standard sigmoid function, with a slope parameter $\lambda = 1$ and an offset $h = 0$.

Calculation of the updated value $a_1^{(1)}$ for C_1:

The updated value $a_1^{(1)}$ of C_1 is computed as follows:

$$a_1^{(1)} = f\left(\left(a_4^{(0)} \otimes w_{4,1}\right) \oplus a_1^{(0)}\right) = f\left(([0.5, 0.7] \otimes [0.5, 0.7]) \oplus [0.6, 0.8]\right).$$

First, we perform the multiplication of interval-valued fuzzy sets (see Eq (2.2)):

$$[0.5, 0.7] \otimes [0.5, 0.7] = [0.5 \times 0.5, \max(0.5 \times 0.7, 0.7 \times 0.5)] = [0.25, 0.35].$$

Next, we apply the addition operation for interval-valued fuzzy sets (see Eq (2.1)):

$$[0.25, 0.35] \oplus [0.6, 0.8] = [\min(0.25 + 0.8, 0.35 + 0.6), 0.35 + 0.8] = [0.95, 1.15].$$

Finally, we apply the activation function:

$$f(0.95) = \frac{1}{1 + e^{-0.95}} \approx 0.71, \quad f(1.15) = \frac{1}{1 + e^{-1.15}} \approx 0.76.$$

Thus, $a_1^{(1)} = [0.71, 0.76]$. *The update process for* C_2 *and* C_3 *follows the same approach as for* C_1, *yielding* $a_2^{(1)} = [0.66, 0.70]$ *and* $a_3^{(1)} = [0.45, 0.60]$. *In contrast, updating* C_4 *is more complex due to the presence of three incoming edges, requiring the aggregation of all causal influences.*

Calculation of the updated value $a_4^{(1)}$ *for* C_4*:*

$$\begin{aligned} a_4^{(1)} &= f\left(\left(a_1^{(0)} \otimes w_{1,4}\right) \oplus \left(a_2^{(0)} \otimes w_{2,4}\right) \oplus \left(a_3^{(0)} \otimes w_{3,4}\right) \oplus a_4^{(0)}\right) \\ &= f\left(([0.6, 0.8] \otimes [0.3, 0.5]) \oplus ([0.3, 0.5] \otimes [-0.4, -0.2])\right. \\ &\quad \left. \oplus ([0.4, 0.6] \otimes [-0.5, -0.4]) \oplus [0.5, 0.7]\right) \\ &= f\left([0.18, 0.3] \oplus [-0.12, -0.06] \oplus [-0.2, -0.16] \oplus [0.5, 0.7]\right) \\ &= f\left([0.58, 0.78]\right) \end{aligned}$$

Finally, the activation function is applied to calculate $a_4^{(1)}$*:* $f(0.58) = \frac{1}{1+e^{-0.58}} \approx 0.67$, $f(0.78) = \frac{1}{1+e^{-0.78}} \approx 1$. *Thus,* $a_4^{(1)} = [0.67, 0.71]$.

Theorem 2. *For an IVFCM with a monotonically non-decreasing activation function, consider two state sequences,* $\{A_t\}$ *and* $\{B_t\}$, *such that for all nodes i and time steps t, the interval of* A_i^t *is entirely contained within that of* B_i^t *(i.e.,* $A_i^t \subseteq B_i^t$*). Additionally, assume that the weight intervals of all edges satisfy* $w_{ij}^L \geq 0$ *and* $w_{ij}^U \geq 0$. *Under these conditions, at time* $t + 1$, *the state interval of each node j remains contained within the corresponding interval in* $\{B_t\}$, *i.e.,* $A_j^{t+1} \subseteq B_j^{t+1}$.

Proof. 1) Inclusiveness of the product operation

For any nodes i and j, since $w_{ij}^L \geq 0$ and $A_i^t \subseteq B_i^t$ (i.e., $A_i^{t,L} \leq B_i^{t,L}$ and $A_i^{t,U} \leq B_i^{t,U}$), the definition of the product operation yields:

$$W_{ij} \otimes A_i^t = \left[w_{ij}^L \cdot A_i^{t,L}, \max\left(w_{ij}^L \cdot A_i^{t,U}, w_{ij}^U \cdot A_i^{t,L}\right)\right].$$

Similarly, for $W_{ij} \otimes B_i^t$, the lower bound is $w_{ij}^L \cdot B_i^{t,L}$, and the upper bound is $\max\left(w_{ij}^L \cdot B_i^{t,U}, w_{ij}^U \cdot B_i^{t,L}\right)$.

Since $w_{ij}^L \cdot A_i^{t,L} \leq w_{ij}^L \cdot B_i^{t,L}$ and

$$\max\left(w_{ij}^L \cdot A_i^{t,U}, w_{ij}^U \cdot A_i^{t,L}\right) \leq \max\left(w_{ij}^L \cdot B_i^{t,U}, w_{ij}^U \cdot B_i^{t,L}\right),$$

it follows that $W_{ij} \otimes A_i^t \subseteq W_{ij} \otimes B_i^t$.

2) Inclusiveness of the addition operation

Since all intervals of $W_{ij} \otimes A_i^t$ are contained within $W_{ij} \otimes B_i^t$, their accumulation satisfies:

$$\bigoplus_{i \neq j} W_{ij} \otimes A_i^t \subseteq \bigoplus_{i \neq j} W_{ij} \otimes B_i^t.$$

Moreover, adding the current states A_j^t and B_j^t, with $A_j^t \subseteq B_j^t$, ensures—by the monotonicity of the addition operation—that:

$$\left(\bigoplus_{i \neq j} W_{ij} \otimes A_i^t \right) \oplus A_j^t \subseteq \left(\bigoplus_{i \neq j} W_{ij} \otimes B_i^t \right) \oplus B_j^t.$$

3) Preservation of the activation function

Since the activation function f is monotonically non-decreasing, an input interval relation $S_A \subseteq S_B$ implies that the output interval satisfies $f(S_A) \subseteq f(S_B)$. Thus,

$$A_j^{t+1} = f(S_A) \subseteq f(S_B) = B_j^{t+1}.$$

In conclusion, the inclusion relation is therefore preserved throughout the iterative inference process of IVFCM. □

Theorem 3. *Suppose the IVFCM satisfies the following conditions:*

1) Parameter convergence: For any concept node A_j with an initial state interval $[x_j^{L(0)}, x_j^{U(0)}]$ and an edge weight interval $[w_{ij}^L, w_{ij}^U]$, there exists a sequence of real numbers $\{\epsilon_k\}$ such that $\epsilon_k \to 0$ and:

$$\forall i, j, \quad |x_j^{L(0)} - x_j^{U(0)}| \leq \epsilon_k, \quad |w_{ij}^L - w_{ij}^U| \leq \epsilon_k.$$

2) Continuity of the activation function: The activation function $f : \mathbb{R} \to \mathbb{R}$ is continuous (e.g., a sigmoid function).

Under these conditions, as $\epsilon_k \to 0$, the inference equation of the IVFCM converges to that of a traditional FCM, i.e.,

$$\lim_{\epsilon_k \to 0} \left[x_j^{L(t)}, x_j^{U(t)} \right] = x_j^{(t)},$$

where the iterative update rule of the traditional FCM is given by

$$x_j^{(t+1)} = f\left(\sum_{i=1}^{N} w_{ij} x_i^{(t)} \right).$$

Proof. For any $t \geq 0$, assume that the interval-valued parameters satisfy

$$\forall i, j, \quad \left| x_j^{L(t)} - x_j^{U(t)} \right| \leq \epsilon_k, \quad \left| w_{ij}^L - w_{ij}^U \right| \leq \epsilon_k,$$

and that there exist real numbers $x_j^{(t)}$ and w_{ij} such that

$$\lim_{\epsilon_k \to 0} x_j^{L(t)} = \lim_{\epsilon_k \to 0} x_j^{U(t)} = x_j^{(t)}, \quad \lim_{\epsilon_k \to 0} w_{ij}^L = \lim_{\epsilon_k \to 0} w_{ij}^U = w_{ij}.$$

Next, verify the degeneracy of interval operations.

(1) Degeneracy of interval addition $\oplus$

For two intervals $[a^L, a^U]$ and $[b^L, b^U]$, addition is defined as

$$[a^L, a^U] \oplus [b^L, b^U] = \left[\min(a^L + b^U, a^U + b^L),\ a^U + b^U\right].$$

When the intervals degenerate into single points (i.e., $a^L = a^U = a$, $b^L = b^U = b$), we obtain

$$[a, a] \oplus [b, b] = [a + b, a + b] = a + b.$$

(2) Degeneracy of interval multiplication $\otimes$

Interval multiplication is defined as

$$[a^L, a^U] \otimes [b^L, b^U] = \left[a^L b^L,\ \max(a^L b^U, a^U b^L)\right].$$

When the intervals degenerate into single points, this reduces to

$$[a, a] \otimes [b, b] = [a \cdot b, a \cdot b] = a \cdot b.$$

(3) Limit interchangeability via continuity of the activation function

Since f is continuous, for any convergent sequence $s_k \to s$, we have

$$\lim_{\epsilon_k \to 0} f\left([s_k^L, s_k^U]\right) = f\left(\lim_{\epsilon_k \to 0} [s_k^L, s_k^U]\right) = f(s).$$

(4) Convergence of the IVFCM

The inference equation of the IVFCM is given by

$$\left[x_j^{L(t+1)}, x_j^{U(t+1)}\right] = f\left(\bigoplus_{i=1}^{N} \left[w_{ij}^L, w_{ij}^U\right] \otimes \left[x_i^{L(t)}, x_i^{U(t)}\right]\right).$$

As $\epsilon_k \to 0$, the interval operations reduce to scalar operations, yielding

$$\bigoplus_{i=1}^{N} \left[w_{ij}^L, w_{ij}^U\right] \otimes \left[x_i^{L(t)}, x_i^{U(t)}\right] \to \sum_{i=1}^{N} w_{ij} x_i^{(t)}.$$

By the continuity of f, it follows that

$$\lim_{\epsilon_k \to 0} \left[x_j^{L(t+1)}, x_j^{U(t+1)}\right] = f\left(\sum_{i=1}^{N} w_{ij} x_i^{(t)}\right) = x_j^{(t+1)}.$$

Applying this process recursively for all t, we conclude that the iterative sequence of the IVFCM converges to the standard FCM. □

Theorem 3 demonstrates that IVFCMs reduce to conventional FCMs as interval widths approach zero. This mathematical property has significant practical implications for model interpretation and application. First, IVFCMs function as an indicator of expert consensus, where interval widths quantify disagreement among experts or data sources; narrowing intervals signify increasing consensus. Theorem 3 ensures a smooth transition to deterministic FCM behavior as consensus emerges. Second, IVFCMs provide a mechanism for model validation. During inference, shrinking interval widths indicate reduced system uncertainty and heightened prediction confidence. Conversely, expanding intervals signal compounding uncertainties or potential system instability, offering critical insights for decision-making. Thus, Theorem 3 not only mathematically bridges IVFCMs and FCMs but also enhances the interpretability and practical utility of interval-based modeling in real-world applications.

4. Convergence of interval-valued fuzzy cognitive maps

From a mathematical perspective, an FCM is a nonlinear dynamic system represented as a directed and weighted fuzzy graph. Its state updates iteratively, with each iteration computed based on the previous activation values and the weight matrix until a stopping condition is met. After multiple iterations, the system's state vector may reach one of the following three states [12]:

Fixed point: If there exists an iteration t_α such that $A^{(t+1)} = A^{(t)}$ for all $t \geq t_\alpha$, the FCM stabilizes at a fixed state, meaning $A^{(t_\alpha)} = A^{(t_\alpha+1)} = A^{(t_\alpha+2)} = \ldots$.

Limit cycle: If there exist integers t_α and P such that $A^{(t+P)} = A^{(t)}$ for all $t \geq t_\alpha$, the FCM exhibits periodic behavior, cycling through a finite set of states. That is, $A^{(t_\alpha)} = A^{(t_\alpha+P)} = A^{(t_\alpha+2P)} = \cdots = A^{(t_\alpha+jP)}$, where $t_\alpha + jP \leq T$ and $j \in \{1, 2, \ldots, T-1\}$.

Chaos: If the state vector changes unpredictably in each iteration, the FCM is in a chaotic regime, indicating neither stability nor periodicity.

The convergence of an FCM refers to its tendency to reach a stable state, either as a fixed point or a limit cycle. Specifically, if the system's output ceases to change significantly or exhibits periodic behavior beyond a certain iteration, it is considered convergent. Analyzing convergence helps assess whether the model effectively captures the underlying system dynamics and provides insights into its mathematical properties and long-term behavior. In an IVFCM, the convergence of the state vector is not merely the approach to a fixed value but also involves the stabilization of interval variations. This means that as iterations progress, the interval values of the concept nodes gradually stabilize and eventually converge to a fixed range, which can be determined by analyzing the upper and lower bounds of the node states. Consequently, when the system converges, the equation

$$\lim_{k\to\infty} d\left(A^{(k)}, A^*\right) = 0$$

holds, where $A^* = \left[[\underline{A_1^*}, \overline{A_1^*}], \ldots, [\underline{A_n^*}, \overline{A_n^*}]\right]^T$, and d is an interval distance metric, such as the Hausdorff distance. As a complex dynamic system, the convergence of an FCM is primarily influenced by multiple factors, including initial conditions, the weight matrix, and the type of activation function. Regarding activation functions, discrete functions (such as binary and ternary functions) do not produce chaotic outputs, whereas nonlinear continuous functions (such as the sigmoid and hyperbolic functions) may introduce convergence challenges under certain conditions. This study focuses on analyzing the convergence of the IVFCM model using the sigmoid activation function.

Theorem 4. *Let $I(\mathbb{R})$ denote the set of all closed intervals on the real number axis, equipped with the metric induced by the Hausdorff distance d_H. For any closed intervals $[a, b], [c, d] \in I(\mathbb{R})$, it is defined as*

$$d_H([a, b], [c, d]) = \max\{|a - c|, |b - d|\}.$$

Let $\mathcal{X} = I(\mathbb{R})^n$ denote the set of all vectors composed of n closed intervals, that is, each element $A \in \mathcal{X}$ has the form $A = ([a_1, b_1], \ldots, [a_n, b_n])$, where $[a_i, b_i] \in I(\mathbb{R})$. Define the metric on $\mathcal{X}$ as

$$d(A, A') = \max_{1\leq i\leq n} d_H([a_i, b_i], [a_i', b_i']),$$

Then $(\mathcal{X}, d)$ forms a complete metric space.

Proof. First, verify that d is a metric:

Non-negativity: Since $d_H([a_i, b_i], [a_i', b_i']) \geq 0$ for each i, its maximum value $d(A, A') \geq 0$.

Identity: If $d(A, A') = 0$, then for all i, $d_H([a_i, b_i], [a_i', b_i']) = 0$, which means $[a_i, b_i] = [a_i', b_i']$, so $A = A'$. Conversely, if $A = A'$, then the Hausdorff distance of each component is 0, so $d(A, A') = 0$.

Symmetry: Since $d_H([a_i, b_i], [a_i', b_i']) = d_H([a_i', b_i'], [a_i, b_i])$, and the symmetry is still maintained after taking the maximum value, we have

$$d(A, A') = d(A', A).$$

Triangle inequality: For each component i, the Hausdorff distance satisfies the triangle inequality:

$$d_H([a_i, b_i], [a_i'', b_i'']) \leq d_H([a_i, b_i], [a_i', b_i']) + d_H([a_i', b_i'], [a_i'', b_i'']).$$

Therefore,

$$\max_i d_H([a_i, b_i], [a_i'', b_i'']) \leq \max_i \left(d_H([a_i, b_i], [a_i', b_i']) + d_H([a_i', b_i'], [a_i'', b_i''])\right).$$

Since $\max_i(x_i + y_i) \leq \max_i x_i + \max_i y_i$, we can obtain

$$d(A, A'') \leq d(A, A') + d(A', A'').$$

So, d is a metric on $\mathcal{X}$.

Next, verify that $(\mathcal{X}, d)$ is a complete metric space.

Let $\{A_k\} = \{([a_1^{(k)}, b_1^{(k)}], \ldots, [a_n^{(k)}, b_n^{(k)}])\}$ be a Cauchy sequence in $\mathcal{X}$. We need to prove that there exists $A \in \mathcal{X}$ such that $A_k \to A$.

Convergence of the component sequences:

For each component i, the sequence $\{[a_i^{(k)}, b_i^{(k)}]\}$ is a Cauchy sequence in $I(\mathbb{R})$. Because for any $\epsilon > 0$, there exists K such that when $k, m \geq K$,

$$d(A_k, A_m) = \max_{1 \leq j \leq n} d_H([a_j^{(k)}, b_j^{(k)}], [a_j^{(m)}, b_j^{(m)}]) < \epsilon.$$

In particular, for the component i, we have

$$d_H([a_i^{(k)}, b_i^{(k)}], [a_i^{(m)}, b_i^{(m)}]) < \epsilon,$$

that is, $\{a_i^{(k)}\}$ and $\{b_i^{(k)}\}$ are Cauchy sequences in $\mathbb{R}$. Since $\mathbb{R}$ is complete, there exist $a_i, b_i \in \mathbb{R}$ such that

$$\lim_{k \to \infty} a_i^{(k)} = a_i, \quad \lim_{k \to \infty} b_i^{(k)} = b_i.$$

Therefore, the closed interval $[a_i, b_i]$ is the limit of the sequence $\{[a_i^{(k)}, b_i^{(k)}]\}$.

Construct the limit element A: Define $A = ([a_1, b_1], \ldots, [a_n, b_n])$. Obviously, $A \in \mathcal{X}$.

Verify $A_k \to A$:

For any $\epsilon > 0$, there exists K_i such that when $k \geq K_i$,

$$|a_i^{(k)} - a_i| < \epsilon, \quad |b_i^{(k)} - b_i| < \epsilon.$$

Take $K = \max_{1\le i\le n} K_i$. When $k \ge K$, for all i, we have

$$d_H([a_i^{(k)}, b_i^{(k)}], [a_i, b_i]) = \max\{|a_i^{(k)} - a_i|, |b_i^{(k)} - b_i|\} < \epsilon.$$

Therefore,

$$d(A_k, A) = \max_{1\le i\le n} d_H([a_i^{(k)}, b_i^{(k)}], [a_i, b_i]) < \epsilon.$$

That is, $A_k \to A$.

In conclusion, $(\mathcal{X}, d)$ is a complete metric space. □

The Hausdorff distance was selected for interval convergence analysis in this paper due to its unique capacity to quantify the worst-case deviation between interval-valued state vectors. This property is essential for IVFCMs, where both bound stability and uncertainty propagation must be jointly evaluated. First, stability in IVFCMs requires the convergence of both lower and upper bounds. The Hausdorff metric ensures boundary-sensitive convergence, unlike midpoint-based metrics that may indicate convergence while bounds oscillate—for example, the intervals $[0, 1]$ and $[0.5, 0.5]$ share a midpoint of 0.5 but exhibit divergent boundary behavior. Second, the Hausdorff metric satisfies all conditions for Banach's fixed-point theorem, including completeness, contraction mapping requirements, and norm-equivalent properties essential for matrix analysis.

Definition 5 (Conservative spectral radius)**.** *For an IVFCM with interval-valued weight matrix* $W = \left([w_{ij}^L, w_{ij}^U]\right)_{n\times n}$*, the conservative spectral radius is defined as:*

$$\rho_{\max}(W) = \max\left\{\rho(|W^L|), \rho(|W^U|)\right\},$$

where $|W^L| = (|w_{ij}^L|)_{n\times n}$ *and* $|W^U| = (|w_{ij}^U|)_{n\times n}$ *are the absolute value matrices of the lower and upper bound weights, and* $\rho(\cdot)$ *denotes the spectral radius.*

This metric represents the worst-case connectivity strength in the system by considering the maximum possible spectral radius across all weight realizations within the intervals.

Theorem 5. *For an IVFCM with the activation function being the sigmoid function, its weight matrix is denoted as* $W = \left([w_{ij}^L, w_{ij}^U]\right)_{n\times n}$*, and its conservative spectral radius is defined as:*

$$\rho_{max}(W) = \max\left\{\rho\left(|W^L|\right), \rho\left(|W^U|\right)\right\},$$

where $|W^L| = \left(|w_{ij}^L|\right)_{n\times n}$, $|W^U| = \left(|w_{ij}^U|\right)_{n\times n}$*, and* $\rho(\cdot)$ *represents the spectral radius of a matrix.*

If $\rho_{max}(W) < \frac{4}{\lambda}$ *is satisfied, then for any initial state vector* $A^{(0)}$*, the iterative sequence* $\{A^{(k)}\}$ *of the IVFCM converges to a unique fixed point* A^* *in the Hausdorff metric space.*

Proof. Let $\mathcal{X}$ be the set consisting of all n-dimensional interval-valued vectors, and define the metric:

$$d(A, A') = \max_{1\le i\le n} d_H\left(A_i, A_i'\right),$$

where $d_H([a, b], [c, d]) = \max\{|a - c|, |b - d|\}$ is the Hausdorff distance.

The iterative equation of the IVFCM is:

$$A_i^{(k+1)} = f\left(\sum_{j=1}^{n} [w_{ij}^L, w_{ij}^U] \otimes A_j^{(k)}\right), \quad i = 1, 2, \ldots, n,$$

where $\otimes$ is the interval multiplication operation.

Linearize the system around the fixed point A^* to obtain the Jacobian matrix J:

$$J = \left(\frac{\partial A_i^{(k+1)}}{\partial A_j^{(k)}} \right)_{n \times n}.$$

Since the derivative of the sigmoid function is:

$$f'(x) = \lambda f(x)(1 - f(x)) \leq \frac{\lambda}{4},$$

the elements of the Jacobian matrix satisfy:

$$J_{ij} = f' \left(\sum_{j=1}^{n} w_{ij} A_j^* \right) \cdot w_{ij}.$$

Therefore, the bounds of the Jacobian matrix are:

$$|J_{ij}| \leq \frac{\lambda}{4} |w_{ij}|.$$

So, the spectral radius of the Jacobian matrix satisfies:

$$\rho(J) \leq \rho \left(\frac{\lambda}{4} |W| \right) = \frac{\lambda}{4} \rho(|W|),$$

where $|W|$ is the absolute value matrix of the weight matrix. To ensure local stability (i.e., $\rho(J) < 1$), it is necessary to satisfy:

$$\frac{\lambda}{4} \rho(|W|) < 1 \quad \Rightarrow \quad \rho(|W|) < \frac{4}{\lambda}.$$

Further considering the conservativeness of the interval-valued weights, define:

$$\rho_{\max}(W) = \max \left\{ \rho(|W^L|), \rho(|W^U|) \right\},$$

and then the convergence condition is revised to:

$$\rho_{\max}(W) < \frac{4}{\lambda}.$$

Define the mapping $G : \mathcal{X} \to \mathcal{X}$ as:

$$G(A)_i = f \left(\sum_{j=1}^{n} [w_{ij}^L, w_{ij}^U] \otimes A_j \right).$$

Combined with the completeness of the Hausdorff distance (according to Theorem 4), prove that G is a contraction mapping.

$$d(G(A), G(A')) \leq \frac{\lambda}{4} \rho_{\max}(W) \cdot d(A, A').$$

When $\rho_{\max}(W) < \frac{4}{\lambda}$, the contraction constant $c = \frac{\lambda}{4} \rho_{\max}(W) < 1$, which satisfies the contraction mapping theorem.

So, according to the Banach fixed-point theorem, there exists a unique $A^* \in \mathcal{X}$ such that $G(A^*) = A^*$, and the iterative sequence converges. □

Theorem 5 establishes the convergence of the IVFCM under specific conditions by leveraging the Banach fixed-point theorem and matrix analysis theory. The convergence of the interval-valued states is assessed using the Hausdorff distance metric. To guarantee convergence, the theorem imposes a spectral radius constraint on the weight matrix, requiring $\rho_{\max}(W) < 4/\lambda$, thereby introducing a design safety margin. In practical applications, this condition can be met by adjusting the slope λ of the activation function or by pruning excessively large weights, thus preventing system divergence caused by high weight magnitudes or overly sensitive activation functions. The validity and convergence behavior of Theorem 5 are further demonstrated through a numerical example.

Example 2. *Suppose there exists an interval-valued fuzzy cognitive map with three concept nodes A_1, A_2, and A_3, and the activation function is $f(x) = \frac{1}{1+e^{-x}}$ (that is, $\lambda = 1$). Its weight matrix is:*

$$W = \begin{pmatrix} [0,0] & [0.2,0.3] & [-0.4,-0.2] \\ [-0.3,-0.1] & [0,0] & [0.1,0.2] \\ [0.3,0.5] & [-0.5,-0.3] & [0,0] \end{pmatrix}.$$

The initial state vector is $A^{(0)} = ([0.5,0.7],[0.3,0.5],[0.4,0.6])^T$.

Compute absolute matrices:

$$|W^L| = \begin{pmatrix} 0 & 0.2 & 0.4 \\ 0.3 & 0 & 0.1 \\ 0.3 & 0.5 & 0 \end{pmatrix}, \quad |W^U| = \begin{pmatrix} 0 & 0.3 & 0.2 \\ 0.1 & 0 & 0.2 \\ 0.5 & 0.3 & 0 \end{pmatrix}.$$

*Calculate spectral radii**:*
(1)Eigenvalues of $|W^L|$: $0.722, -0.461, -0.261 \rightarrow \rho(|W^L|) = 0.722$.
(2)Eigenvalues of $|W^U|$: $0.619, -0.310, -0.309 \rightarrow \rho(|W^U|) = 0.619$.
Then,

$$\rho_{\max}(W) = \max(0.722, 0.619) = 0.722.$$

Verify convergence condition:

$$\rho_{\max}(W) = 0.722 < \frac{4}{\lambda} = 4 \quad (\textit{condition satisfied}).$$

Next, the first five iterations of this case model are executed through programming in the Python programming language to demonstrate the gradual convergence process of the state intervals. The results of these iterations are presented in Table 1.

Table 1. Verification of convergence under the conditions of Theorem 5.

Iteration number	A_1	A_2	A_3	$d(A^{(k)}, A^{(k-1)})$
0	[0.5000, 0.7000]	[0.3000, 0.5000]	[0.4000, 0.6000]	-
1	[0.5225, 0.5424]	[0.4875, 0.5075]	[0.4650, 0.4900]	0.1200
2	[0.5215, 0.5458]	[0.4811, 0.5043]	[0.4722, 0.4982]	0.0173
3	[0.5229, 0.5468]	[0.4801, 0.5037]	[0.4719, 0.4980]	0.0014
4	[0.5230, 0.5468]	[0.4802, 0.5038]	[0.4718, 0.4979]	0.0001
5	[0.5230, 0.5468]	[0.4802, 0.5038]	[0.4718, 0.4979]	< 0.00001

In Example 2, the spectral radius condition of Theorem 5 holds ($\rho_{\max}(W) \approx 0.722 < 4$), and the system actually converges by iteration 5.

The convergence guarantee in Theorem 5, grounded in the Banach fixed-point theorem framework, relies on two assumptions: the sigmoid slope constraint ($\lambda < 4/\rho_{\max}(W)$) and the establishment of a complete metric space via the Hausdorff distance (Theorem 4). The condition $\rho_{\max}(W) < 4/\lambda$ aligns with real-world stability requirements, though it may appear restrictive for highly connected systems (e.g., neural networks with $\rho_{\max}(W) \approx 5$–10) or systems with strong feedback. When these conditions are violated, three implementation strategies prove effective:

1) Slope adjustment: Increase λ to sharpen sigmoid responses, though values > 2 risk oversimplifying dynamics.

2) Weight regularization: Scale weights via $W' = \alpha W$ (with $\alpha < 4/(\lambda\rho_{\max}(W))$ or prune weak edges ($|w_{ij}| < \delta$).

3) Architecture modification: Decompose connected components or introduce damping factors.

The analysis and demonstration in this section provide theoretical support for the stability of IVFCMs in practical applications, such as economic systems, medical diagnosis, social decision-making, etc. It can guide the design of model parameters, optimize the value range of the weight matrix, and ensure that the model will not exhibit divergent or chaotic behaviors during the inference process.

5. Centrality measures of interval-valued fuzzy cognitive maps

Research on centrality measures for IVFCMs remains at the forefront of the field, with the interval-valued fuzzy nature of node states and causal edge weights requiring further in-depth investigation. This study introduces two novel centrality measurement methods tailored to the mathematical characteristics of IVFCMs. By adhering strictly to the principles of interval arithmetic and incorporating newly defined operations—such as the absolute value of interval-valued fuzzy numbers and the ordering of path weights—this work establishes a computational framework that balances mathematical rigor with practical applicability.

Existing centrality measures for standard FCMs [15, 19–22] typically operate on crisp weights and cannot directly handle interval-valued uncertainties. While a few studies [19–22] have explored centrality in fuzzy graphs, they either ignore directionality or collapse intervals into scalars, losing uncertainty information. The proposed measures address these gaps by: (1) defining interval-specific operations (e.g., absolute value in Def. 6) to preserve uncertainty semantics; (2) incorporating directionality and the sign of causal influences via interval arithmetic; and (3) introducing global influence propagation metrics (closeness centrality) that account for interval attenuation (Theorem 6). This represents the first mathematically rigorous framework for centrality analysis in IVFCMs.

5.1. Degree centrality of interval-valued fuzzy cognitive maps

In a weighted directed graph, the degree centrality of a node is defined as the sum of its in-degree and out-degree centralities. The in-degree centrality is calculated as the sum of the weights of edges directed toward the node, while the out-degree centrality is the sum of the weights of edges originating from the node. In IVFCMs, edge weights represent causal influences and may take on positive or negative values, corresponding to promoting or inhibiting effects, respectively. Using these original

weight values directly can result in semantic inconsistencies and computational errors. To address this, the degree centrality in IVFCMs is computed by summing the absolute values of the interval weights of both incoming and outgoing edges. The following section defines the method for representing interval absolute values.

Definition 6 (Interval absolute value)**.** *For any interval-valued causal edge weight* $[a, b]$*, its absolute value is defined as:*

$$|[a,b]| = \begin{cases} [\min(|a|,|b|), \max(|a|,|b|)] & \text{if } a \cdot b \geq 0, \\ [0, \max(|a|,|b|)] & \text{otherwise}. \end{cases}$$

Definition 7 (Degree centrality of interval-valued fuzzy cognitive map)**.** *In an IVFCM, the degree centrality (IV-DC) of the node* A_j *characterizes its local influence by summing the interval absolute values of the weights of all directly connected edges (both incoming and outgoing):*

$$\textit{IV-DC}(A_j) = \bigoplus_{i=1, i\neq j}^{N} \left(\left| [w_{ij}^L, w_{ij}^U] \right| \oplus \left| [w_{ji}^L, w_{ji}^U] \right| \right),$$

where N *is the total number of nodes, and* $[w_{ij}^L, w_{ij}^U]$ *is the interval-valued fuzzy number of the edge weight from the node* A_i *to* A_j*. The operator* $\oplus$ *represents interval addition as defined in Definition 3.*

Example 3. *Taking the economic system IVFCM in Figure 1 as an example, calculate the degree centrality of node* C_1 *(economic growth):*

The weights of incoming edges: The weight of $C_4 \to C_1$ *is* $[0.5, 0.7]$*, and the absolute value is* $[0.5, 0.7]$.

The weights of outgoing edges: The weight of $C_1 \to C_2$ *is* $[0.4, 0.6]$*, the weight of* $C_1 \to C_3$ *is* $[-0.5, -0.3]$*, and the weight of* $C_1 \to C_4$ *is* $[0.3, 0.5]$*. Their absolute values are* $[0.4, 0.6]$*,* $[0.5, 0.3]$*, and* $[0.3, 0.5]$*, respectively.*

Calculation of degree centrality:

$$\begin{aligned} \textit{IV - DC}(C_1) &= [0.5, 0.7] \oplus ([0.4, 0.6] \oplus [0.3, 0.5] \oplus [0.3, 0.5]) \\ &= [0.5, 0.7] \oplus [1.4, 1.6] \\ &= [2.1, 2.3]. \end{aligned}$$

The results show that the economic growth node (C_1) *has a relatively high direct influence in the economic system.*

Degree centrality is one of the most widely used and conceptually straightforward measures of centrality in network analysis. It evaluates a node's level of activity from a local perspective by quantifying the strength of its direct connections to other nodes. Nodes with a greater number of connections are generally regarded as more influential within the network. For example, in the IVFCM model of an ecosystem, a species node with high degree centrality indicates direct interactions with numerous other species. The strength of these interactions—expressed as interval values—reflects the species' potential role in local energy flow and material cycling. However, because degree centrality considers only immediate connections, it neglects indirect paths and broader structural features of the network. Consequently, it may fail to fully capture a node's importance in more complex network configurations.

5.2. Closeness centrality of interval-valued fuzzy cognitive maps

Closeness centrality is a widely used centrality measure that quantifies the proximity of a given node to all other nodes in a network. It is often interpreted as an indicator of the time required for information to spread from one node to all reachable nodes. A higher closeness centrality implies a shorter average distance to other nodes, suggesting that the node may play a more influential role in information dissemination or the transmission of causal effects. As a global centrality measure, its calculation relies on complete knowledge of the network's overall structure.

In a conventional weighted network, the closeness centrality of a node u is defined as:

$$CC(u) = \left[\sum_{\forall v} d^w(u, v)\right]^{-1}, \tag{5.1}$$

where $d^w(u, v)$ denotes the shortest weighted distance between nodes u and v. However, in IVFCMs, edge weights do not represent distances but instead indicate the strength of causal influence. Directly applying Eq (5.1) in this context would incorrectly interpret causal influence as spatial distance, thereby failing to capture a node's true influence on others. For instance, in the IVFCM modeling an economic system, a strong positive causal influence—such as the impact of high investment on economic growth—might be misrepresented as a "long distance" under the traditional metric. In reality, this relationship signifies a strong promotive effect, which cannot be accurately reflected through the concept of distance. In IVFCMs, a node's importance lies in its ability to transmit causal influence efficiently and effectively to other nodes. Therefore, the notion of closeness centrality should be redefined in terms of both the intensity of causal influence and the efficiency of its propagation. According to Definition 6, the absolute value of an edge weight in an IVFCM reflects the strength of causal influence, providing a basis for this redefinition.

Definition 8 (Causal influence strength of a single acyclic path)**.** *In an IVFCM, for all acyclic paths $P(u, v)$ from node u to v, the causal influence strength of path p is defined as the product of the absolute values of the edge weights along the path:*

$$I(p) = \bigotimes_{(i,j)\in p} |w_{ij}|,$$

where w_{ij} is the interval-valued weight from node i to node j, that is, $[w_{ij}^-, w_{ij}^+]$. $|w_{ij}|$ is the absolute value of the interval, and $\bigotimes$ represents the interval-valued multiplication operation.

Theorem 6. *In an IVFCM, consider an acyclic path $p = (u = i_1, i_2, \ldots, i_k = v)$ between any two nodes u and v. Let the edge weights along path p be given by the intervals $[w_{i_1i_2}^L, w_{i_1i_2}^U], [w_{i_2i_3}^L, w_{i_2i_3}^U], \ldots, [w_{i_{k-1}i_k}^L, w_{i_{k-1}i_k}^U]$, with their corresponding absolute interval values denoted as $|[w_{i_1i_2}^L, w_{i_1i_2}^U]|, |[w_{i_2i_3}^L, w_{i_2i_3}^U]|, \ldots, |[w_{i_{k-1}i_k}^L, w_{i_{k-1}i_k}^U]|$. Define the causal influence strength of path p as*

$$I(p) = \bigotimes_{j=1}^{k-1} \left|[w_{i_ji_{j+1}}^L, w_{i_ji_{j+1}}^U]\right|.$$

If there exists a subpath $p' = (u = i_1, i_2, \ldots, i_m = v)$ of p with $m < k$, and its causal influence strength is defined as

$$I(p') = \bigotimes_{j=1}^{m-1} \left|[w_{i_ji_{j+1}}^L, w_{i_ji_{j+1}}^U]\right|,$$

then it holds that $I(p) \subseteq I(p')$. That is, in an IVFCM, the causal influence strength along a single acyclic path attenuates progressively.

Proof. Let the path $p = (u = i_1, i_2, \ldots, i_k = v)$, and let $p' = (u = i_1, i_2, \ldots, i_m = v)$ with $m < k$ be a sub-path of p.

The causal influence strength $I(p)$ of the path p is obtained by successively performing interval multiplications. Suppose that the product of the absolute values of the intervals corresponding to the first $m-1$ edges has been computed as:

$$I(p'') = \bigotimes_{j=1}^{m-1} \left|[w^L_{i_j i_{j+1}}, w^U_{i_j i_{j+1}}]\right| = [x^L, x^U],$$

and the absolute value of the interval for the m-th edge is given by

$$\left|[w^L_{i_m i_{m+1}}, w^U_{i_m i_{m+1}}]\right| = [y^L, y^U].$$

According to the rules of interval multiplication, the overall influence strength is

$$I(p) = \bigotimes_{j=1}^{k-1} \left|[w^L_{i_j i_{j+1}}, w^U_{i_j i_{j+1}}]\right| = I(p'') \otimes [y^L, y^U] = [x^L y^L, \max(x^L y^U, x^U y^L)].$$

Given that $0 \leq x^L \leq x^U \leq 1$ and $0 \leq y^L \leq y^U \leq 1$, it follows that $x^L y^L \leq x^L \leq x^U$, and $\max(x^L y^U, x^U y^L) \leq x^U$. Specifically, when $y^L = y^U = 1$, we have $\max(x^L y^U, x^U y^L) = x^U$; otherwise, the inequality is strict.

Therefore, $I(p) \subseteq I(p'')$, and since $I(p'') = I(p')$, it follows that $I(p) \subseteq I(p')$.

This completes the proof. □

Theorem 6 demonstrates that in IVFCMs, the strength of causal influence gradually diminishes as the length of an acyclic path increases. According to Definition 8, the path with the greatest influence—that is, the path with the highest $I(p)$—is identified as the dominant influence from node u to node v. Furthermore, only acyclic paths are considered when computing causal influence strength, in order to eliminate interference from feedback loops.

Definition 9 (Closeness centrality of interval-valued fuzzy cognitive map)**.** *In an IVFCM, the closeness centrality of a node u is defined as the sum of the maximum causal influence intensities on all other nodes:*

$$C_C^{IVFCM}(u) = \bigoplus_{\forall v \neq u} \max_{p \in P(u,v)} I(p)$$

where $\bigoplus$ represents the interval-valued addition operation.

According to Definition 8, all acyclic paths from u to v must be traversed. In the worst-case scenario, such as a fully connected graph, the number of paths grows factorially as $O((n-2)!)$, resulting in a time complexity of $O(n!)$. This exponential growth renders the conventional computation method impractical for large-scale networks. To address this, path search optimization is essential. The following strategies can be employed:

1) Limit path length: In real-world systems, the influence of longer paths typically diminishes significantly. By setting a maximum path length $L \ll n$, the complexity can be reduced to $O(n^2 \cdot n^L)$.

2) Enhanced Dijkstra algorithm: A modified version of the Dijkstra algorithm can be used to identify dominant paths by maximizing the product of causal influences, leveraging its greedy approach.

3) Dynamic programming: Exploit the overlapping subproblem structure by caching previously computed path influences, thereby eliminating redundant calculations.

Algorithm 1 presents a pseudocode implementation of IVFCMs closeness centrality measure, optimized using Dijkstra's algorithm. The algorithm's time complexity is primarily determined by the computation of the maximum causal influence paths between node pairs. To this end, Dijkstra's algorithm, enhanced with a priority queue, is employed to compute the maximum product path for each node pair, achieving a time complexity of $O(M + N \log N)$ per computation. Since this process must be repeated for all N^2 node pairs, the overall time complexity of Algorithm 1 is $O(N^2(M + N \log N))$. The space complexity is $O(N^2)$, attributed to the auxiliary space required to store the maximum path influence values for all node pairs. These analyses demonstrate that the proposed framework is scalable for moderate-sized networks ($N \leq 200$) and provides a roadmap for optimizing larger systems.

Algorithm 1 The calculation process of closeness centrality for IVFCMs

Require: The adjacency matrix W of the IVFCM, the nodes set V
Ensure: The closeness centrality C of each node

for Each node $u \in V$ **do**
  $C[u] \leftarrow [0, 0]$ ▷ Initialize the interval value
  for Each node $v \in V \setminus \{u\}$ **do**
    $max\_inf \leftarrow [0, 0]$ ▷ Record the maximum path influence
    Use the improved Dijkstra's algorithm to find the maximum product path p^* from u to v
    $I(p^*) \leftarrow \bigotimes_{(i,j)\in p^*} |W[i, j]|$
    $max\_inf \leftarrow \max_{\text{Hausdorff}}(max\_inf, I(p^*))$
    $C[u] \leftarrow C[u] \oplus max\_inf$ ▷ Interval addition
  end for
end for
return C

In the conventional Dijkstra algorithm, the greedy strategy selects, at each step, the node with the smallest cumulative distance from the starting point. In contrast, within IVFCMs, the objective is to identify the path with the maximum causal influence, defined as the maximum interval product along the path. To accommodate this, an enhanced version of Dijkstra algorithm employs a modified greedy strategy: each node's priority is determined by the upper bound of the interval representing the influence strength from the node to the starting point. The path with the largest upper bound is treated as the current optimal path, and the neighbors of the corresponding node are explored first. When a new path is found, its cumulative interval product is computed and compared with existing paths using Hausdorff-based interval comparison. If the new path has a higher upper bound, it replaces the current best path. Notably, because interval multiplication is non-monotonic (e.g., $[0.5, 0.7] \otimes [0.4, 0.6] = [0.2, 0.42]$), the algorithm must dynamically maintain all cumulative interval products to ensure that no potentially optimal paths are overlooked.

The closeness centrality of an IVFCM should emphasize the efficiency with which nodes transmit influence through causal chains. By redefining this centrality in terms of maximum path influence

intensity and interval operations—incorporating causal effectiveness transformation and interval aggregation rules—this method addresses the mismatch between traditional distance metrics and causal semantics. It preserves the intuitiveness of conventional centrality measures while accommodating the dynamic characteristics of fuzzy cognitive maps. This approach effectively identifies key nodes within the IVFCM on a global scale, offering a novel quantitative tool for analyzing complex systems.

Algorithm 2 Dijkstra's algorithm based on the maximum causal influence path

Require: Adjacency matrix W (edge weights are interval values), starting node u
Ensure: The maximum product path $I_{\max}(u, v)$ from u to all nodes

```
Initialize the priority queue Q to store nodes and their current maximum product intervals
Initialize I_max(u, u) ← [1, 1], and for other nodes I_max(u, v) ← [0, 0]
Add the starting node u to Q with the priority I_max(u, u).upper = 1
while Q is not empty do
    Extract the node current with the highest priority (the largest upper bound) from Q
    for Each neighbor node v ∈ Adj(current) do
        Calculate the product of the new path: I_new = I_max(u, current) ⊗ |W[current][v]|
        if I_new.upper > I_max(u, v).upper then
            Update I_max(u, v) ← I_new
            Add v to Q with the priority of I_new.upper
        end if
    end for
end while
return I_max(u, v) for all v
```

Example 4. *Taking the economic system IVFCM in Figure 1 as an example, calculate the closeness centrality of nodes C_1 (economic growth), C_2 (inflation), C_3 (unemployment rate), and C_4 (consumer confidence):*

Taking the calculation of the closeness centrality of node C_1 (economic growth) as an example, first calculate the causal influence strength of a single acyclic path:

From C_1 to C_2: The edge weight is $[0.4, 0.6]$*, the absolute value of the interval is* $[0.4, 0.6]$*, and the causal influence strength* $I(p_{12}) = [0.4, 0.6]$*;*

From C_1 to C_3: The edge weight is $[-0.5, -0.3]$*, the absolute value of the interval is* $[0.3, 0.5]$*, and the causal influence strength* $I(p_{13}) = [0.3, 0.5]$*;*

From C_1 to C_4: For the direct path $C_1 \to C_4$, the edge weight is $[0.3, 0.5]$*, the absolute value of the interval is* $[0.3, 0.5]$*, and the causal influence strength* $I(p_{14}^1) = [0.3, 0.5]$*. For the indirect path $C_1 \to C_2 \to C_4$, the weight of $C_1 \to C_2$ is* $[0.4, 0.6]$*, and the weight of $C_2 \to C_4$ is* $[-0.4, -0.2]$*. First calculate the absolute values of the intervals, which are* $[0.4, 0.6]$ *and* $[0.2, 0.4]$*, respectively. According to the interval value multiplication operation rule, the causal influence strength of this indirect path* $I(p_{14}^2) = [0.4, 0.6] \otimes [0.2, 0.4] = [0.40.2, \max(0.40.4, 0.60.2)] = [0.08, 0.16]$*. Compare* $I(p_{14}^1)$ *and* $I(p_{14}^2)$*, and compare the upper bounds. Since* $0.5 > 0.16$*, the direct path is better. So the maximum causal influence strength from C_1 to C_4 is* $[0.3, 0.5]$.

Then, according to the interval value addition operation rule, calculate the closeness centrality of

node C_1:

$$\begin{aligned} C_C^{IVFCM}(C_1) &= [0.4, 0.6] \oplus [0.3, 0.5] \oplus [0.3, 0.5] \\ &= [\min(0.4 + 0.5, 0.6 + 0.3), 0.6 + 0.5] \oplus [0.3, 0.5] \\ &= [\min(0.9 + 0.5, 1.1 + 0.3), 1.1 + 0.5] \\ &= [1.4, 1.6]. \end{aligned}$$

Through a similar calculation process, the closeness centrality of C_2, C_3, and C_4 can be obtained. The full centrality measures for all nodes are summarized in Table 2.

Table 2. Closeness centrality measures of each node in the numerical case 1.

Node	Closeness centrality interval	Maximum causal influence path
C_1	$[1.4, 1.6]$	$C_1 \to C_2$, $C_1 \to C_3$, $C_1 \to C_4$
C_4	$[1.05, 1.25]$	$C_4 \to C_1$, $C_4 \to C_1 \to C_2$, $C_4 \to C_1 \to C_3$
C_2	$[0.46, 0.66]$	$C_2 \to C_4$, $C_2 \to C_4 \to C_1$, $C_2 \to C_4 \to C_1 \to C_3$
C_3	$[0.8, 0.9]$	$C_3 \to C_4$, $C_3 \to C_4 \to C_1$, $C_3 \to C_4 \to C_1 \to C_2$

As illustrated in the numerical example 4, node C_1 is directly connected to C_2, C_3, and C_4, with relatively large edge weights in absolute value. Consequently, its closeness centrality is the highest, within the interval $[1.4, 1.6]$. This suggests that the economic growth node exerts a broad influence on the overall economic system. It is evident that nodes with numerous direct connections and high edge weights typically serve as central hubs in causal propagation. In contrast, C_2 and C_3 each have only a single outgoing edge and transmit influence primarily through indirect paths. Due to path length, the product interval diminishes, resulting in lower closeness centrality values ($[0.46, 0.66]$ for C_2 and $[0.8, 0.9]$ for C_3). These findings support Theorem 6, demonstrating that longer paths reduce the product interval and diminish the influence of peripheral nodes.

This subsection systematically investigates methods for quantifying node importance in IVFCMs using centrality indicators. As a fundamental tool in complex network analysis, centrality measures must be adapted to account for the interval-valued fuzzy nature of causal edge weights in IVFCMs. The proposed measures provide three key advancements over existing FCM centrality methods: (1) Faithful uncertainty propagation through interval arithmetic operations; (2) causal-semantic consistency via absolute-value transformations and influence-strength metrics; and (3) computational feasibility for interval-optimized path analysis. This enables robust identification of pivotal nodes in uncertain systems. In practical applications, it is essential to consider multiple centrality metrics to capture node importance and influence from diverse perspectives within complex networks.

6. A case study on time series prediction

To validate the superior capability of the IVFCM model in addressing challenges such as knowledge representation of uncertain information and noise interference, this section presents a case study on an IVFCM-based interval prediction method for time series. First, the fuzzy information granulation method is employed to transform the original time series data into a triangular fuzzy number time

series, extracting the fuzzy features of the data. This provides an interval-valued data format with richer semantic information, enhancing the representational capacity for complex real-world scenarios. Next, the triangular fuzzy numbers are converted into interval numbers via the α-cut method, and these interval numbers are clustered using the Hausdorff distance-based interval-valued fuzzy C-means clustering algorithm, with the cluster centers designated as the conceptual nodes of the IVFCM. Subsequently, the edge weights of the IVFCM are learned from experimental data through the particle swarm optimization (PSO) algorithm, ultimately constructing an IVFCM-based time series model for interval prediction. Experimental results demonstrate that the IVFCM-related model excels in interval prediction tasks, exhibiting significant advantages in handling uncertainty, capturing semantic information, and ensuring the accuracy of prediction intervals.

In terms of experimental data acquisition, this case study selected three publicly available time series datasets from diverse domains for the experiments. These datasets include the daily closing price of Tesla stock (TSLA), the total daily electricity consumption across Germany (Elec.), and the daily minimum temperature data for Boston, USA (Temp.).

In time series forecasting tasks, commonly used evaluation metrics include mean absolute error (MAE), root mean square error (RMSE), and mean absolute percentage error (MAPE). However, in interval-valued forecasting tasks, both the ground truth data and the model's predicted outputs are interval-valued. Therefore, the aforementioned traditional regression metrics need to be adapted to accommodate the interval characteristics. Below are the designed evaluation metrics for interval-valued time series forecasting models:

$$\mathrm{MAE}_{\mathrm{interval}} = \frac{1}{2N}\sum_{i=1}^{N}\left(|L_{\mathrm{true}}^{(i)} - L_{\mathrm{pred}}^{(i)}| + |U_{\mathrm{true}}^{(i)} - U_{\mathrm{pred}}^{(i)}|\right), \tag{6.1}$$

$$\mathrm{RMSE}_{\mathrm{interval}} = \frac{1}{2}\left(\left(\frac{1}{N}\sum_{i=1}^{N}\left(L_{\mathrm{true}}^{(i)} - L_{\mathrm{pred}}^{(i)}\right)^2\right)^{\frac{1}{2}} + \left(\frac{1}{N}\sum_{i=1}^{N}\left(U_{\mathrm{true}}^{(i)} - U_{\mathrm{pred}}^{(i)}\right)^2\right)^{\frac{1}{2}}\right), \tag{6.2}$$

$$\mathrm{MAPE}_{\mathrm{interval}} = \frac{1}{2}\left(\frac{100}{N}\sum_{i=1}^{N}\frac{\left|U_{\mathrm{true}}^{(i)} - U_{\mathrm{pred}}^{(i)}\right|}{\left|U_{\mathrm{true}}^{(i)}\right|} + \frac{100}{N}\sum_{i=1}^{N}\frac{\left|L_{\mathrm{true}}^{(i)} - L_{\mathrm{pred}}^{(i)}\right|}{\left|L_{\mathrm{true}}^{(i)}\right|}\right). \tag{6.3}$$

Here, $L_{\mathrm{true}}, U_{\mathrm{true}}$ and $L_{\mathrm{pred}}, U_{\mathrm{pred}}$ represent the lower and upper bounds of the true interval and the predicted interval, respectively, and N denotes the number of samples. To verify the predictive ability of the proposed time-series interval prediction model, the proposed model was compared with several classical prediction models. These comparative models include the autoregressive integrated moving average model (ARIMA) based on statistical methods, the first-order fuzzy time series model (FTS), the conventional fuzzy cognitive map model (FCM), the high-order fuzzy cognitive map model (high-order FCM) [35] and the bidirectional long short-term memory model (BLSTM) [36].

As indicated in Table 3, the IVFCM model achieved optimal or suboptimal performance across the financial market (TSLA), power consumption (Elec.), and temperature prediction (Temp.) datasets. Among the nine evaluated indicators spanning these three datasets, the IVFCM attained the best performance in six cases (66.7%). These results demonstrate the model's adaptability to interval prediction tasks for diverse time series data, highlighting its robust cross-domain generalization

capabilities. Furthermore, the IVFCM utilizes an interval-valued state update rule; its iterative inference process enhances prediction transparency.

Table 3. Comparative experimental results.

Dataset	Metrics	ARIMA	FTS	FCM	High-Order FCM	BLSTM	Proposed model
TSLA	MAE	61.12	41.12	51.05	38.31	40.77	**35.12**
	RMSE	70.33	51.30	61.16	49.57	51.17	**48.34**
	MAPE	15.11	11.37	12.23	9.83	**8.18**	8.32
Elec.	MAE	80.68	80.82	70.85	55.08	60.61	**50.56**
	RMSE	94.95	91.06	88.96	75.32	78.70	**72.63**
	MAPE	12.86	12.07	8.63	5.56	**5.17**	5.94
Temp.	MAE	2.85	3.12	3.10	2.75	2.87	**2.27**
	RMSE	4.03	3.61	3.71	3.52	3.56	**3.35**
	MAPE	5.26	5.22	4.83	**3.86**	5.17	4.08

7. Conclusions

This study systematically explores the theoretical foundations, inference mechanisms, convergence properties, and centrality measurement approaches of interval-valued fuzzy cognitive maps (IVFCMs), addressing critical gaps in understanding their mathematical characteristics and dynamic behavior. By extending traditional fuzzy cognitive maps (FCMs), IVFCMs utilize interval-valued fuzzy numbers to represent concept states and causal weights, thereby enhancing their ability to model uncertainty and complexity in dynamic systems.

Regarding the inference mechanism, the study details the process of updating node state values using interval-valued fuzzy operations, illustrated through an economic system example. The inference process entails computing causal influences via interval multiplication, aggregating multi-path effects through interval addition, and subsequently applying an activation function to normalize the results within a bounded interval (e.g., [0, 1]). As a nonlinear dynamic system, the convergence behavior of IVFCMs is affected by factors such as initial conditions, the weight matrix, and the choice of activation function. To address this, a convergence theorem is proposed based on the spectral radius of the weight matrix, derived using the Banach fixed-point theorem and matrix analysis. Furthermore, the study introduces novel centrality measurement methods tailored to the interval-valued fuzzy nature of IVFCMs. Specifically, enhanced degree and closeness centrality metrics are proposed to more effectively identify key nodes within the network. Empirical validation on time series prediction confirmed IVFCMs' superiority in handling uncertainty, achieving optimal performance across financial, energy, and temperature datasets. This underscores the framework's versatility and robustness.

Despite these strengths, the IVFCM framework exhibits three key limitations. First, its convergence behavior and prediction accuracy are sensitive to initial interval widths: Excessively wide intervals may propagate overestimation errors during state transitions, while overly narrow intervals could inadequately capture epistemic uncertainty. Second, interval arithmetic operations (especially multiplication) may introduce information loss due to the dependency problem, where repeated

operations artificially inflate interval widths and obscure causal relationships. Third, in sparse or highly uncertain datasets (e.g., domains with scarce expert knowledge or noisy measurements), weight learning and convergence may become unstable as interval-valued parameters lack sufficient constraints to guide meaningful inferences.

Future research should focus on improving the scalability, robustness, and adaptability of FCMs by incorporating advances in artificial intelligence. One promising direction is the integration of multi-source data, enabling the fusion of structured data (e.g., numerical tables) and unstructured data (e.g., text and images) to uncover latent causal relationships. Another important area involves further analysis of the stability and reliability of FCMs and their variants under varying conditions. Through mathematical modeling and empirical validation, future studies may investigate performance in the presence of data noise, parameter perturbations, and structural changes, ultimately aiming to establish more general convergence criteria. Additionally, integrating FCMs with machine learning techniques—such as using learning algorithms to automatically infer model structure and parameters—could significantly enhance modeling efficiency and predictive accuracy.

Author contributions

Jindong Feng and Zengtai Gong: Conceptualization, Methodology, Validation, Writing–original draft, Writing–review & editing. The final version of the manuscript was read and approved by all authors.

Use of Generative-AI tools declaration

The authors declare that they have not used Artificial Intelligence (AI) tools in the creation of this article.

Acknowledgments

The authors would like to express their thanks to the editors of the journal and the referees for their careful reading of the manuscript and providing many helpful comments and suggestions which improved the presentation of the paper. This work is supported by the National Natural Science Foundation of China (12471444).

Conflict of interest

The authors hereby declare that there is no conflict of interest.

References

1. B. Kosko, Fuzzy cognitive maps, *International Journal of Man-Machine Studies*, **24** (1986), 65–75. https://doi.org/10.1016/S0020-7373(86)80040-2
2. E. Bakhtavar, M. Valipour, S. Yousefi, R. Sadiq, K. Hewage, Fuzzy cognitive maps in systems risk analysis: a comprehensive review, *Complex Intell. Syst.*, **7** (2021), 621–637. https://doi.org/10.1007/s40747-020-00228-2

3. A. Mourhir, Scoping review of the potentials of fuzzy cognitive maps as a modeling approach for integrated environmental assessment and management, *Environ. Modell. Softw.*, **135** (2021), 104891. https://doi.org/10.1016/j.envsoft.2020.104891
4. S. Habib, M. Akram, Medical decision support systems based on fuzzy cognitive maps, *Int. J. Biomath.*, **12** (2019), 1950069. https://doi.org/10.1142/S1793524519500694
5. C. Borrero-Domínguez, T. Escobar-Rodríguez, Decision support systems in crowdfunding: a fuzzy cognitive maps (FCM) approach, *Decis. Support Syst.*, **173** (2023), 114000. https://doi.org/10.1016/j.dss.2023.114000
6. H. A. Choukolaei, S. E. Mirani, M. Hejazi, P. Ghasemi, A GIS-based crisis management using fuzzy cognitive mapping: PROMETHEE approach (a potential earthquake in Tehran), *Soft Comput.*, in press. https://doi.org/10.1007/s00500-023-09260-z
7. H. A. Choukolaei, S. E. Mirani, P. Ghasemi, M. J. Rezaee, System dynamics simulation follow-up fuzzy cognitive map for investigating the effect of risks on relief in crisis management, *Eng. Appl. Artif. Intel.*, **136** (2024), 109002. https://doi.org/10.1016/j.engappai.2024.109002
8. O. Orang, P. C. de Lima e Silva, F. G. Guimarães, Time series forecasting using fuzzy cognitive maps: a survey, *Artif. Intell. Rev.*, **56** (2023), 7733–7794. https://doi.org/10.1007/s10462-022-10319-w
9. Y. Boutalis, T. L. Kottas, M. Christodoulou, Adaptive estimation of fuzzy cognitive maps with proven stability and parameter convergence, *IEEE Trans. Fuzzy Syst.*, **17** (2009), 874–889. https://doi.org/10.1109/TFUZZ.2009.2017519
10. T. Kottas, Y. Boutalis, M. Christodoulou, Bi-linear adaptive estimation of fuzzy cognitive networks, *Appl. Soft Comput.*, **12** (2012), 3736–3756. https://doi.org/10.1016/j.asoc.2012.01.025
11. C. J. K. Knight, D. J. B. Lloyd, A. S. Penn, Linear and sigmoidal fuzzy cognitive maps: an analysis of fixed points, *Appl. Soft Comput.*, **15** (2014), 193–202. https://doi.org/10.1016/j.asoc.2013.10.030
12. G. Nápoles, E. Papageorgiou, R. Bello, K. Vanhoof, On the convergence of sigmoid fuzzy cognitive maps, *Inform. Sciences*, **349** (2016), 154–171. https://doi.org/10.1016/j.ins.2016.02.040
13. C. Luo, X. Song, Y. J. Zheng, Algebraic dynamics of k-valued fuzzy cognitive maps and its stabilization, *Knowl. Based Syst.*, **209** (2020), 106424. https://doi.org/10.1016/j.knosys.2020.106424
14. I. Á. Harmati, M. F. Hatwágner, L. T. Kóczy, Global stability of fuzzy cognitive maps, *Neural Comput. Appl.*, **35** (2023), 7283–7295. https://doi.org/10.1007/s00521-021-06742-9
15. L. C. Freeman, D. Roeder, R. R. Mulholland, Centrality in social networks: II. experimental results, *Soc. Networks*, **2** (1979), 119–141. https://doi.org/10.1016/0378-8733(79)90002-9
16. K. Das, S. Samanta, M. Pal, Study on centrality measures in social networks: a survey, *Soc. Netw. Anal. Min.*, **8** (2018), 13. https://doi.org/10.1007/s13278-018-0493-2
17. M. Jalili, A. Salehzadeh-Yazdi, S. Gupta, O. Wolkenhauer, M. Yaghmaie, O. Resendis-Antonio, et al., Evolution of centrality measurements for the detection of essential proteins in biological networks, *Front. Physiol.*, **7** (2016), 375. https://doi.org/10.3389/fphys.2016.00375

18. P. D. Meo, K. Musial-Gabrys, D. Rosaci, G. M. L. Sarnè, L. Aroyo, Using centrality measures to predict helpfulness-based reputation in trust networks, *ACM Trans. Internet Techn.*, **17** (2017), 8. https://doi.org/10.1145/2981545

19. R.-J. Hu, Q. Li, G.-Y. Zhang, W.-C. Ma, Centrality measures in directed fuzzy social networks, *Fuzzy Inf. Eng.*, **7** (2015), 115–128. https://doi.org/10.1016/j.fiae.2015.03.008

20. Z. Lu, Q. Zhang, X. Du, D. Wu, F. Gao, A fuzzy social network centrality analysis model for interpersonal spatial relations, *Knowl. Based Syst.*, **105** (2016), 206–213. https://doi.org/10.1016/j.knosys.2016.05.020

21. M. Obiedat, S. Samarasinghe, A novel semi-quantitative Fuzzy Cognitive Map model for complex systems for addressing challenging participatory real life problems, *Appl. Soft Comput.*, **48** (2016), 91–110. https://doi.org/10.1016/j.asoc.2016.06.001

22. Q. Wang, Z. T. Gong, Structural centrality in fuzzy social networks based on fuzzy hypergraph theory, *Comput. Math. Organ. Theory*, **26** (2020), 236–254. https://doi.org/10.1007/s10588-020-09312-x

23. W. Stach, L. Kurgan, W. Pedrycz, Higher-order fuzzy cognitive maps, In: *NAFIPS 2006 - 2006 Annual meeting of the North American fuzzy information processing society*, Montreal, QC, Canada, 03–06 June 2006, 166–171. https://doi.org/10.1109/NAFIPS.2006.365402

24. H. A. Mohammadi, S. Ghofrani, A. Nikseresht, Using empirical wavelet transform and high-order fuzzy cognitive maps for time series forecasting, *Appl. Soft Comput.*, **135** (2023), 109990. https://doi.org/10.1016/j.asoc.2023.109990

25. X. Li, Y. Ma, Q. Zhou, X. Zhang, Sparse large-scale high-order fuzzy cognitive maps guided by spearman correlation coefficient, *Appl. Soft Comput.*, **167** (2024), 112253. https://doi.org/10.1016/j.asoc.2024.112253

26. D. K. Iakovidis, E. Papageorgiou, Intuitionistic fuzzy cognitive maps for medical decision making, *IEEE Trans. Inf. Technol. Biomed.*, **15** (2010), 100–107. https://doi.org/10.1109/TITB.2010.2093603

27. L. Sha, Y. Shao, Y. Li, A framework of fermatean fuzzy cognitive map and its extension based on Hamacher operation, *Eng. Appl. Artif. Intel.*, **136** (2024), 108676. https://doi.org/10.1016/j.engappai.2024.108676

28. P. Hajek, O. Prochazka, Interval-valued fuzzy cognitive maps for supporting business decisions, In: *2016 IEEE international conference on fuzzy systems (FUZZ-IEEE)*, Vancouver, BC, Canada, 24–29 July 2016, 531–536. https://doi.org/10.1109/FUZZ-IEEE.2016.7737732

29. J. Aguilar, A dynamic fuzzy-cognitive-map approach based on random neural networks, *International Journal of Computational Cognition*, **1** (2003), 91–107.

30. T. Hickey, Q. Ju, M. H. Van Emden, Interval arithmetic: from principles to implementation, *J. ACM*, **48** (2001), 1038–1068. https://doi.org/10.1145/502102.502106

31. G. Deschrijver, Arithmetic operators in interval-valued fuzzy set theory, *Inform. Sciences*, **177** (2007), 2906–2924. https://doi.org/10.1016/j.ins.2007.02.003

32. A. Piegat, L. Dobryakova, A decomposition approach to type 2 interval arithmetic, *Int. J. Appl. Math. Comput. Sci.*, **30** (2020), 185–201. https://doi.org/10.34768/amcs-2020-0015

33. P. Breiding, K. Rose, S. Timme, Certifying zeros of polynomial systems using interval arithmetic, *ACM Trans. Math. Softw.*, **49** (2023), 11. https://doi.org/10.1145/3580277

34. M. B. Gorzałczany, A method of inference in approximate reasoning based on interval-valued fuzzy sets, *Fuzzy Set Syst.*, **21** (1987), 1–17. https://doi.org/10.1016/0165-0114(87)90148-5

35. D. Shan, L. Wang, W. Lu, J. Chen, Convex optimization based high-order fuzzy cognitive map modeling and its application in time series predicting, *IEEE Access*, **12** (2024), 12683–12698. https://doi.org/10.1109/ACCESS.2024.3355194

36. A. Saeed, C. Li, M. Danish, S. Rubaiee, G. Tang, Z. Gan, Hybrid bidirectional LSTM model for short-term wind speed interval prediction, *IEEE Access*, **8** (2020), 182283–182294. https://doi.org/10.1109/ACCESS.2020.3027977

AIMS Press